

Crack-size dependence of fracture toughness in transformation-toughened ceramics

YASURO IKUMA*, ANIL V. VIRKAR

Department of Materials Science and Engineering, University of Utah, Salt Lake City, Utah 84112, USA

Fracture toughness (K_{IC}) has been determined for Y_2O_3 -partially stabilized zirconia, Y_2O_3 -partially stabilized hafnia, CaO-partially stabilized zirconia and $Al_2O_3 + ZrO_2$ composites. It is shown that K_{IC} determined using the indentation technique may not yield a unique number but may depend upon the crack size (C) (on the indent load). The slope of K_{IC} against $C^{1/2}$ yields the magnitude of the surface stress created by the tetragonal \rightarrow monoclinic transition on the surface induced by grinding. K_{IC} determined using the double cantilever beam (DCB) technique, on the other hand, is shown to be independent of crack length.

1. Introduction

It is well known that several ceramics with metastably retained particles of tetragonal zirconia exhibit considerably higher values of fracture toughness and fracture strength compared to similar ceramics containing the cubic form of zirconia [1]. Enhancement of toughness and strength is attributed to martensitic-type transformation of tetragonal zirconia to its low temperature, low density monoclinic polymorph in the neighbourhood of a crack tip. This type of toughening, termed transformation toughening, has been documented in many ceramics, e.g. MgO-partially stabilized zirconia (MgO-PSZ) [2], Y_2O_3 -PSZ [3], CaO-PSZ [4], transformation-toughened Al_2O_3 [5, 6], β'' - Al_2O_3 [7, 8] to name a few. Numerous models have been proposed which semiquantitatively account for most of the salient features of transformation toughening [9–12]. It is also well known that in transformation-toughened ceramics which are surface ground, tetragonal \rightarrow monoclinic transformation occurs in the near surface region. Since monoclinic zirconia is a lower density phase, upon transformation a compressive stress develops in the near surface region which

leads to an increase in the stress required for fracture from surface flaws.

In many studies on transformation-toughened ceramics, the fracture toughness, K_{IC} , is determined using the indentation technique [13]. The zone of surface compression is expected to influence K_{IC} measured using this technique. The objective of this work is to show that K_{IC} determined using the indentation technique on transformation-toughened ceramics may not yield a unique value, but that K_{IC} so determined may be crack-length dependent. Furthermore, information on the variation of K_{IC} (measured by indentation) with crack length can be used to estimate the magnitude of surface residual stress along similar lines shown by Marshall and Lawn [14] who estimated surface stress in glass.

In this paper fracture toughness measurements on Y_2O_3 -PSZ, CaO-PSZ, Y_2O_3 -PS hafnia and transformation-toughened alumina are reported. K_{IC} has been primarily measured using the indentation technique although a few measurements have been conducted using the double cantilever beam (DCB) technique.

*Present address: Ikutoku Institute of Technology, Kanagawa, Japan.

2. Theory

Lawn and co-workers [15–17] have shown that for the residual crack system that develops under a Vickers indenter, the stress intensity factor, K_I , is given by

$$K_I = \chi \frac{P}{C^{3/2}} \quad (1)$$

where P is the load, C is the crack radius (assuming a half-penny shaped crack) and χ is the proportionality constant. If a surface residual stress (assumed to extend to a depth greater than C) of magnitude σ_R exists, then the stress intensity is given by

$$K_I = \chi \frac{P}{C^{3/2}} + \sigma_R \frac{2}{\pi^{1/2}} C^{1/2} \quad (2)$$

The crack would extend when $K_I = K_{IC}^0$. Thus, if the indentation load is P_c , the resulting crack size is given by

$$K_{IC}^0 = \chi \frac{P_c}{C^{3/2}} + \sigma_R \frac{2}{\pi^{1/2}} C^{1/2} \quad (3)$$

in which K_{IC}^0 is the true fracture toughness (in the absence of surface residual stress).

The apparent or the effective fracture toughness is

$$K_{IC} = \frac{\chi P_c}{C^{3/2}} \quad (4)$$

Therefore

$$K_{IC} = K_{IC}^0 - \sigma_R \frac{2}{\pi^{1/2}} C^{1/2} \quad (5)$$

in which K_{IC} is the apparent K_{IC} measured based on the indentation load and the corresponding crack size. Equation 5 suggests that K_{IC} measured using the indentation technique is linearly proportional to $C^{1/2}$ with slope $= -\sigma_R(2/\pi^{1/2})$. For a compressive stress, $\sigma_R < 0$ and K_{IC} increases with increasing C . To examine whether K_{IC} determined using the indentation technique depends upon the crack size, experiments were conducted using several transformation toughened ceramics.

3. Experimental procedure

3.1. Specimen fabrication

Four ceramic systems were chosen: Y_2O_3 -PSZ; Y_2O_3 -HfO₂; Al_2O_3 + ZrO₂; and CaO-PSZ.

3.1.1. Y_2O_3 -PSZ

Commercial* yttria stabilized ZrO₂ containing

8 wt% (4.5 mol%) Y_2O_3 was isostatically pressed and sintered in air at 1600°C. The density of the sintered specimens was about 5.7 g cm⁻³. Y_2O_3 -PSZ was not subjected to any additional thermal treatments.

3.1.2. Y_2O_3 -PS hafnia

HfO₂ powder was mechanically mixed with Y_2O_3 for 3 days in a ball mill. Two compositions were chosen: 5.5 and 12 mol% Y_2O_3 . HfO₂ with 12 mol% Y_2O_3 is expected to be all cubic while HfO₂ with 5.5 mol% Y_2O_3 should contain tetragonal zirconia particles in a matrix of cubic zirconia. Specimens were sintered in air at 1700°C (12% Y_2O_3) and 1900°C (5.5% Y_2O_3). A few of the samples containing 5.5% Y_2O_3 were annealed at 1380°C for 7 h. At 1380°C, the stable phases are known to be cubic and the monoclinic polymorphs for a composition containing 5.5 mol% Y_2O_3 .

3.1.3. Al_2O_3 + ZrO₂

Specimens of Al_2O_3 with 10 and 15 vol% ZrO₂ were fabricated by hot-pressing of alumina[†] and zirconia (undoped). Al_2O_3 and ZrO₂ powders were mechanically mixed in a ball mill for 10 h. Hot-pressed specimens were essentially of theoretical density as judged by metallographic examination which indicated porosity less than 1%. Densities of the alumina samples with 10 and 15 vol% ZrO₂ were 4.18 and 4.30 g cm⁻³, respectively. X-ray diffraction indicated the presence of both the tetragonal and the monoclinic ZrO₂ in these specimens. This was attributed to poor mixing which led to the presence of a few large ZrO₂ particles (greater than 2 to 3 μm) that converted to monoclinic upon cooling.

3.1.4. CaO-PSZ

CaCO₃ and ZrO₂ (undoped) were milled in isopropanol for 3 days in a stoichiometry to yield 8.4 mol% CaO. The mixture after drying was calcined at 1100°C. The calcined powder was dry-milled, pressed into rectangular bars and isostatically pressed. Specimens were sintered in air at 1800°C. Density of sintered samples was generally between 5.6 and 5.7 g cm⁻³. Some of the specimens were annealed at 1325°C for up to 1 day.

*Zircar Products, Florida, New York 10921, USA.

†RC-HP, Reynolds.

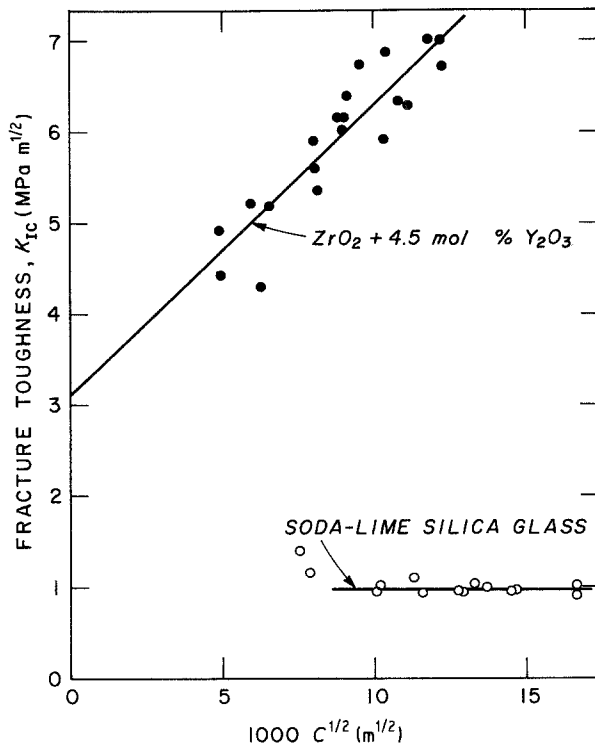


Figure 1 K_{IC} , determined by indentation, plotted against $C^{1/2}$ for Y_2O_3 -PSZ and soda-lime silica glass.

3.2. Measurement of K_{IC}

3.2.1. Indentation

Dense specimens were first surface ground on a 100 μm diamond wheel followed by polishing down to 1 μm . A loading rig for use in conjunction with a universal testing machine[‡] was designed and built. Using a Vickers indenter, samples were indented with loads up to 130 N. Subsequently, samples were examined under an optical microscope to determine the indent and the crack dimensions. By varying the indent load, cracks of various sizes were generated. K_{IC} was determined using the approach given by Evans and Charles [3].

3.2.2. DCB technique

K_{IC} was also determined for Y_2O_3 -PSZ and CaO-PSZ using the DCB technique. Samples with machined notches were first loaded until a sharp crack pops in. The crack length was measured using a fluorescent dye. Samples were subsequently fractured.

4. Results and discussion

K_{IC} of Y_2O_3 -PSZ determined using the indentation technique is plotted against $C^{1/2}$ in Fig. 1.

The K_{IC} is seen to increase linearly with increasing $C^{1/2}$ indicative of a surface compressive stress. From the slope, the magnitude of the compressive stress is estimated to be 282 MPa (40 900 psi). By contrast, K_{IC} plotted against $C^{1/2}$ for annealed soda-lime silica glass also plotted in Fig. 1 shows K_{IC} to be independent of the crack length indicating that the surface stress in the soda-lime silica glass tested was nearly zero. Volume change from tetragonal to monoclinic is known to be about 7%. Using the Young's modulus of Y_2O_3 -PSZ at 145 GN m^{-2} and the compressive stress as 282 MPa, the vol% tetragonal zirconia that transformed into the monoclinic form is calculated to be $\sim 6.25\%$.

The intercept of K_{IC} against $C^{1/2}$ for Y_2O_3 -PSZ gives K_{IC}^0 (equation 5). K_{IC}^0 represents the fracture toughness of Y_2O_3 -PSZ containing the same volume fraction of tetragonal and monoclinic zirconia but with no surface stress. K_{IC}^0 , however, is not the fracture toughness of a pristine unground sample since volume fraction of tetragonal zirconia in the near surface region would be different for unground and ground samples. Upon surface grinding, some of the tetragonal zirconia converts to monoclinic thereby creating a surface

[‡]Model 1125, Instron Corp. Canton, Mass., USA.

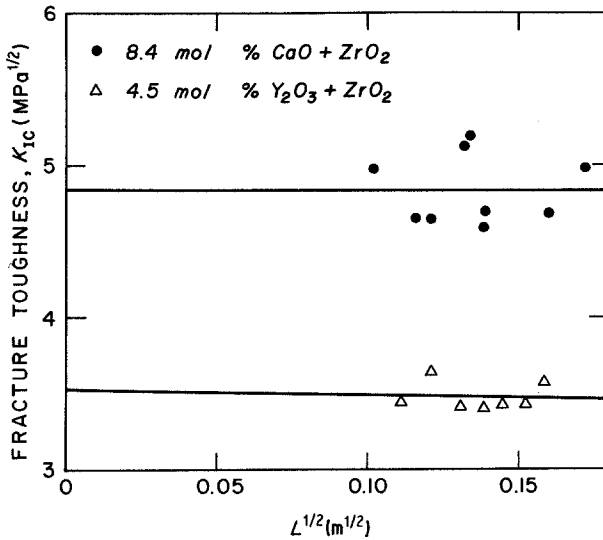


Figure 2 K_{IC} , determined using DCB technique, plotted against $L^{1/2}$ for Y_2O_3 -PSZ and CaO-PSZ.

stress. When indented, some of the remaining tetragonal zirconia may convert into monoclinic zirconia in the stress-field of the crack leading to some transformation toughening which will be reflected in K_{IC}^0 . In total, there are at least three distinct contributions to K_{IC}^0 .

1. transformation toughening due to tetragonal \rightarrow monoclinic phase change;

2. crack interaction (pinning or deflection) with dispersed zirconia particles, and

3. fracture toughness of the matrix-cubic zirconia. If, upon grinding, all of the tetragonal zirconia in the near surface region transforms to the monoclinic polymorph, there would be no contribution from transformation toughening to K_{IC}^0 . In the present experiments, K_{IC}^0 was found to be $3.1 \text{ MPa m}^{1/2}$.

K_{IC} of Y_2O_3 -PSZ determined using a DCB technique is plotted against $L^{1/2}$ (L is the crack length) in Fig. 2. The K_{IC} so determined is similar to K_{IC}^0 except that the contribution of transformation toughening would be expected to be greater due to the fact that the volume fraction of tetragonal zirconia is greater (since the K_{IC} determined from unground DCB samples is not expected to be influenced by surface stress). Thus, K_{IC} is expected to be greater than K_{IC}^0 . Furthermore, as K_{IC} so determined is not influenced by surface stresses, it should be independent of crack length. As shown in Fig. 2, K_{IC} is independent of the crack length L . The average value of K_{IC} determined using the DCB technique was $3.48 \text{ MPa m}^{1/2}$ (which is greater than K_{IC}^0 as to be expected). By

contrast, K_{IC} determined using the indentation technique has yielded values as high as $7 \text{ MPa m}^{1/2}$. Such high values are primarily the result of surface compressive stresses. It is expected that K_{IC} determined using the indentation technique would agree with the DCB data provided polished samples are annealed at a temperature above the monoclinic \rightarrow tetragonal transition temperature prior to indentation. K_{IC} of CaO-PSZ determined using the DCB technique is also shown in Fig. 2. The average value of K_{IC} is $4.85 \text{ MPa m}^{1/2}$, and within the limits of experimental accuracy, K_{IC} is found to be independent of crack length. In CaO-PSZ, K_{IC} could not be determined by indentation due to very large grain size ($\sim 60 \mu\text{m}$).

K_{IC} of HfO_2 with 5.5 and 12 mol% Y_2O_3 determined using the indentation technique is plotted against $C^{1/2}$ in Fig. 3. K_{IC} plotted against $C^{1/2}$ for HfO_2 -5.5% Y_2O_3 , which was rapidly cooled to room temperature upon sintering at 1900°C , exhibits the largest slope (the corresponding residual surface stress being 153 MPa or 22150 psi). After the sample was heat treated at 1380°C for 7 h, K_{IC} was lower although it still increased linearly with $C^{1/2}$. The corresponding surface compressive stress was determined to be 71 MPa or 10260 psi. Heat treatment at 1380°C either converts the tetragonal HfO_2 to its stable monoclinic form, or coarsens the tetragonal HfO_2 so that upon cooling it transforms to the monoclinic polymorph or both. The net effect is to decrease the overall tetragonal HfO_2 content. Consequently, both the slope and the intercept

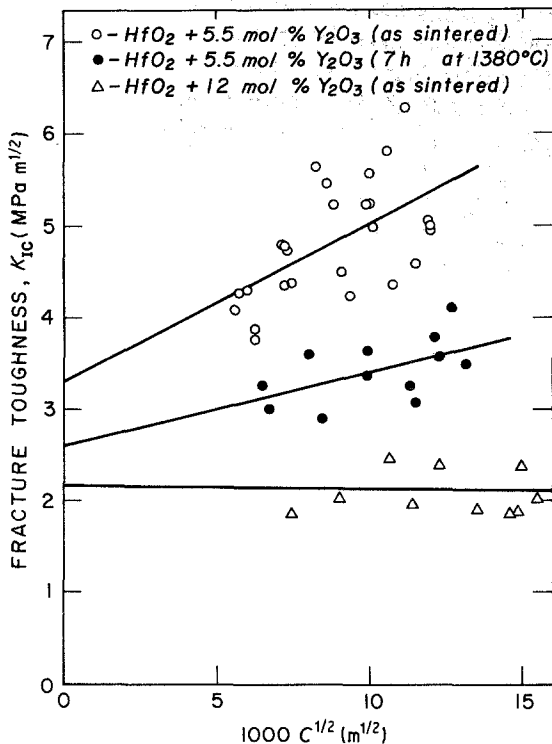


Figure 3 K_{IC} , determined by indentation, plotted against $C^{1/2}$ for Y_2O_3 -PS hafnia.

are lower. (K_{IC}^0 for the as sintered specimens is $3.3 \text{ MPa m}^{1/2}$ while that for the annealed specimens is $2.6 \text{ MPa m}^{1/2}$). The HfO_2 -12% Y_2O_3 sample that was sintered at 1900°C and rapidly cooled to room temperature contained only the cubic form. As is evident from Fig. 3, the K_{IC} determined here is the lowest and, furthermore, is independent of crack length indicating that no residual stress exists. (The least squares fit to the data gave a tensile stress of $\sim 3 \text{ MPa}$ or $\sim 400 \text{ psi}$. Within the limits of experimental scatter, it may be concluded that there is essentially no surface stress.)

In the case of HfO_2 samples also, there are three contributions to K_{IC} discussed previously. As the intrinsic volume change upon tetragonal \rightarrow monoclinic transition is lower in the case of HfO_2 , it is expected that transformation-toughening contribution to K_{IC}^0 will be lower than in the case of Y_2O_3 -PSZ. Furthermore, the magnitude of the surface compressive stress is also expected to be lower than in Y_2O_3 -PSZ. As shown in Figs. 1 and 3, the experimental data are in accord with these expectations.

$K_{IC}-C^{1/2}$ data on hot-pressed Al_2O_3 containing 0, 10 and 15 vol% ZrO_2 are shown in Fig. 4. Once again, K_{IC} plotted against $C^{1/2}$ exhibits the greatest slope for the sample containing 15 vol% ZrO_2 (the corresponding surface residual stress is computed to be 198 MPa or $28\,700 \text{ psi}$). For the sample containing 10 vol% ZrO_2 , the magnitude of the surface residual stress is 148 MPa or $21\,400 \text{ psi}$, while the surface of Al_2O_3 with no ZrO_2 is nearly stress free. If all of the ZrO_2 upon fabrication were in the tetragonal form and if all of it had converted to monoclinic in the near surface region upon grinding, the magnitude of the surface stress would have been 1769 MPa ($257 \times 10^3 \text{ psi}$) for $Al_2O_3 + 15\% ZrO_2$ and 1179 MPa ($171 \times 10^3 \text{ psi}$) for $Al_2O_3 + 10\% ZrO_2$. As the initial mixing of ZrO_2 and Al_2O_3 was not very good, there were large agglomerates of ZrO_2 which upon cooling converted to the monoclinic form. Furthermore, apparently, the grinding process used in this study was essentially not effective enough to convert the rest of the tetragonal zirconia into the monoclinic form. These two factors are responsible for the much lower value of surface compressive stress observed in the present experiments.

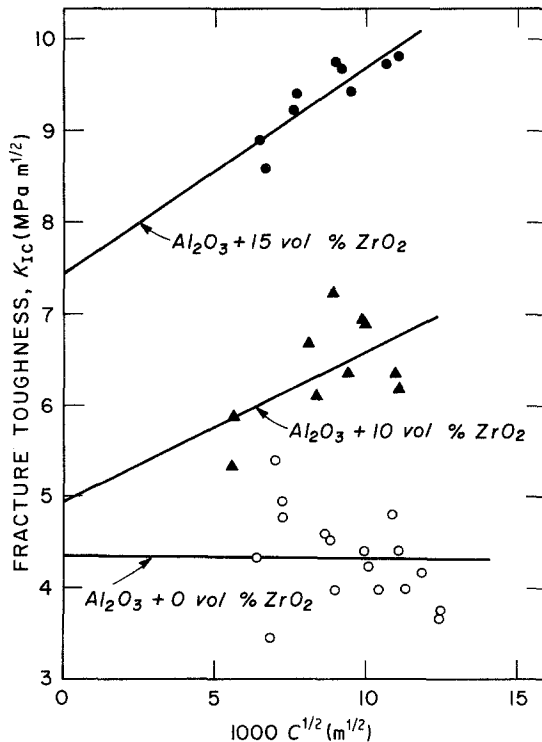


Figure 4 K_{IC} , determined by indentation, plotted against $C^{1/2}$ for Al_2O_3 , $Al_2O_3 + 10 \text{ vol} \% ZrO_2$ and $Al_2O_3 + 15 \text{ vol} \% ZrO_2$.

Assuming that the amount of tetragonal zirconia which converts into monoclinic upon grinding is proportional to the total volume fraction of zirconia, one would expect the magnitude of surface compressive stress in the sample containing 15% ZrO₂ to be 1.5 times than in the sample containing 10% ZrO₂. The experimentally determined ratio of the compressive stresses is 1.34, indicating fair agreement with expectations.

K_{IC}^0 for the Al₂O₃ + ZrO₂ samples increases rapidly with volume fraction of ZrO₂. ($K_{IC}^0 = 4.35 \text{ MPa m}^{1/2}$ for Al₂O₃ + 0% ZrO₂, $K_{IC}^0 = 4.92 \text{ MPa m}^{1/2}$ for Al₂O₃ + 10% ZrO₂ and $K_{IC}^0 = 7.46 \text{ MPa m}^{1/2}$ for Al₂O₃ + 15% ZrO₂). Possibly the contribution of transformation toughening as well as crack-particle interaction toughening is much greater in the sample containing 15% ZrO₂ as compared to the sample containing 10% ZrO₂.

It has been assumed that the entire crack is contained within the zone of compressive residual stresses. The largest crack sizes (C) have been on the order of 225 μm . It is unlikely that the zone of uniform compressive stresses exists to such depths. As this aspect is not taken into account, the incorporation of σ_R into the analysis would be more complicated than indicated by Equation 5. Considerable scatter exhibited by the K_{IC} data also makes it difficult to determine accurately the magnitude of the surface compressive stress from the slope. Possibly an X-ray technique should be used to estimate σ_R for comparative purposes. Despite these shortcomings, the data presented here clearly show that K_{IC} increases linearly with $C^{1/2}$.

5. Conclusions

In transformation-toughened ceramics, fracture toughness determined using the indentation technique may yield values considerably greater than those obtained using a technique such as DCB. Furthermore, the K_{IC} determined may depend upon the crack length (and indirectly on the indentation load.) The principal reason for the apparently high K_{IC} obtained using the indentation technique is the existence of a surface compression zone in transformation-toughened

ceramics which are ground. As pointed out by Marshall and Lawn [14], the indentation technique may be used to determine the magnitude of the surface stress. To determine the true toughness of transformation-toughened ceramics using the indentation technique, it may be necessary to anneal the samples after polishing but prior to indentation.

Acknowledgement

This work was supported by the National Science Foundation under grant number DMR 79-12668.

References

1. R. C. GARVIE, R. H. HANNICK and R. T. PASCOE, *Nature* **258** (1975) 703.
2. D. L. PORTER and A. H. HEUER, *J. Amer. Ceram. Soc.* **60** (1977) 183.
3. F. F. LANGE, *J. Mater. Sci.* **17** (1982) 240.
4. R. C. GARVIE, R. R. HUGHAN and R. T. PASCOE, in "Processing of Crystalline Ceramics", edited by H. Palmour, R. F. Davis and T. M. Hare (Plenum Press, New York, 1977) p. 263.
5. N. CLAUSSEN, *J. Amer. Ceram. Soc.* **59** (1976) 49.
6. F. F. LANGE, *J. Mater. Sci.* **17** (1982) 247.
7. L. VISWANATHAN, Y. IKUMA and A. V. VIRKAR, *ibid.* **18** (1983) 109.
8. F. F. LANGE, B. I. DAVIS and D. O. RALEIGH, *J. Amer. Ceram. Soc.* **66** (1983) C-50.
9. A. G. EVANS and A. H. HEUER, *ibid.* **63** (1980) 241.
10. F. F. LANGE, *J. Mater. Sci.* **17** (1982) 235.
11. D. L. PORTER, A. G. EVANS and A. H. HEUER, *Acta Metall.* **27** (1979) 1649.
12. R. M. McMEEKING and A. G. EVANS, *J. Amer. Ceram. Soc.* **65** (1982) 242.
13. A. G. EVANS and E. A. CHARLES, *ibid.* **59** (1976) 371.
14. D. B. MARSHALL and B. R. LAWN, *ibid.* **60** (1977) 86.
15. B. R. LAWN and E. R. FULLER, *J. Mater. Sci.* **10** (1975) 2016.
16. B. R. LAWN, A. G. EVANS and D. B. MARSHALL, *J. Amer. Ceram. Soc.* **63** (1980) 574.
17. D. B. MARSHALL and B. R. LAWN, *J. Mater. Sci.* **14** (1979) 2001.

Received 22 September
and accepted 4 October 1983